

## ARTICLE OPEN



# Global risk assessment of compound hot-dry events in the context of future climate change and socioeconomic factors

Hossein Tabari<sup>1,2,3</sup> and Patrick Willems<sup>1</sup>

Compound hot-dry events have the potential to cause significant damages and propel socioeconomic systems towards tipping points by overwhelming the ability of natural and human systems to cope with the combined stressors. As climate change continues to alter hazard patterns, the impacts of these events will be further compounded by changes in exposure and vulnerability. However, the future risk of these events and the role of these components remain poorly understood. Using a multimodel ensemble, we find that by the end of the 21st century, an additional 0.7–1.7 billion people globally will be exposed to amplified compound events, depending on the scenarios. Additionally, the cropland exposure to these events is projected to increase by 2–5.7 million km<sup>2</sup>. Our findings also suggest that countries with weak governance will experience a twice larger increase in the risk of compound events than those with good governance. This underscores the importance of effective governance in mitigating and managing the escalating risks of compound events.

*npj Climate and Atmospheric Science* (2023)6:74; <https://doi.org/10.1038/s41612-023-00401-7>

## INTRODUCTION

Compound extreme events have the potential to worsen the damages caused by individual events and push global socioeconomic systems towards tipping points<sup>1,2</sup>. This is because the combined stressors can overwhelm the ability of exposed natural and human systems to cope with extreme conditions<sup>3</sup>. When these stressors take the form of major natural hazards such as drought and heatwaves, which have been responsible for 40% of global disaster-related deaths in recent decades<sup>4</sup>, the impact can be devastating. Examples of the devastating impact of compound events include the 2010 Russia event, which had a death toll of 55,000 people<sup>5</sup>, and the 2018 Europe event, which resulted in a financial loss of approximately 3.3 billion Euros<sup>6</sup>. In addition to the devastating impact on human life and economic systems, compound hot-dry events can negatively affect agriculture by reducing crop yields<sup>7,8</sup>, leading to increased food insecurity in vulnerable regions<sup>9,10</sup>.

To reduce the future socioeconomic impacts of compound hot-dry events, it is important to analyze these events at different spatial and temporal scales. Recent studies have examined the impact of climate change on the probability and frequency of co-occurring hot-dry events, with dry events characterized based on precipitation (meteorological drought)<sup>11–15</sup>. However, the risk of compound hot-dry events changes not only due to the changes in climate events (hazards)<sup>16</sup>, but also in the exposure of people, economic assets, and ecosystems and their vulnerability to hazardous conditions<sup>17</sup>. In this regard, augmented population exposure in hazard-prone areas was found to be a more significant factor than hazard amplification for the future risk increase of some extreme events<sup>18</sup>. The evolving character of the risk components<sup>19–21</sup>, therefore, calls for anticipatory risk management of compound events through proactive, prospective disaster risk reduction (DRR) efforts<sup>22</sup>.

Despite the significant impact of compound hot-dry events on various sectors, their future socioeconomic risk has not been thoroughly investigated. Prior global risk assessments on

individual drought and heatwave events<sup>23–25</sup> potentially underestimated the risk associated with extreme conditions<sup>26</sup>. While a few global-scale studies have examined exposure to compound hot-dry events, they have not considered the role of vulnerability in shaping the risks<sup>13,27,28</sup>. Thus, this study aims to assess global future changes in the risk of compound hot-dry events, taking into account dynamic hazards, exposure, and vulnerability.

To characterize dry events, we use soil moisture as it explicitly represents the core physical processes, including interactions between land surface processes, atmospheric demand, and plants<sup>29,30</sup>. This is in contrast to simple index-based impact models based on precipitation which tend to neglect these critical factors<sup>31,32</sup>. The factors represented by soil moisture are particularly important in analyzing the impact of future compound hot-dry events on various sectors, especially agriculture. The summer 2022 event across Europe, which led to a 16% decrease in crop yield, exemplifies the severe impact on agriculture<sup>33</sup>.

Soil moisture represents water deficits at each location as a function of meteorological conditions, landscape topography, soil characteristics, and crops' physiology<sup>34,35</sup>. Moreover, future global warming is expected to cause a more widespread and intense drying signal for soil moisture than precipitation<sup>36,37</sup>. Therefore, the use of soil moisture in this study is crucial, and it highlights the need to consider the complex interactions between climate, land surface, and agricultural systems.

The historical and future risk of compound hot-dry events is derived as the product of the occurrence probability of compound events (hazard), integrated population and cropland exposure, and the governance indicator (GI<sup>38</sup>) as a proxy for vulnerability and coping capacity. The compound events are quantified based on the Coupled Model Intercomparison Project Phase 6 (CMIP6) simulations from 18 climate models for four Shared Socioeconomic Pathways (SSPs). To prioritize adaptation actions, the projected changes in the risk are decomposed into the changes in hazard, population and crop exposure, and vulnerability.

<sup>1</sup>Department of Civil Engineering, KU Leuven, Leuven, Belgium. <sup>2</sup>Department of Meteorological and Climate Research, Royal Meteorological Institute of Belgium, Uccle, Belgium. <sup>3</sup>Faculty of Applied Engineering, University of Antwerp, Antwerp, Belgium. ✉email: [hossein.tabari@uantwerpen.be](mailto:hossein.tabari@uantwerpen.be)

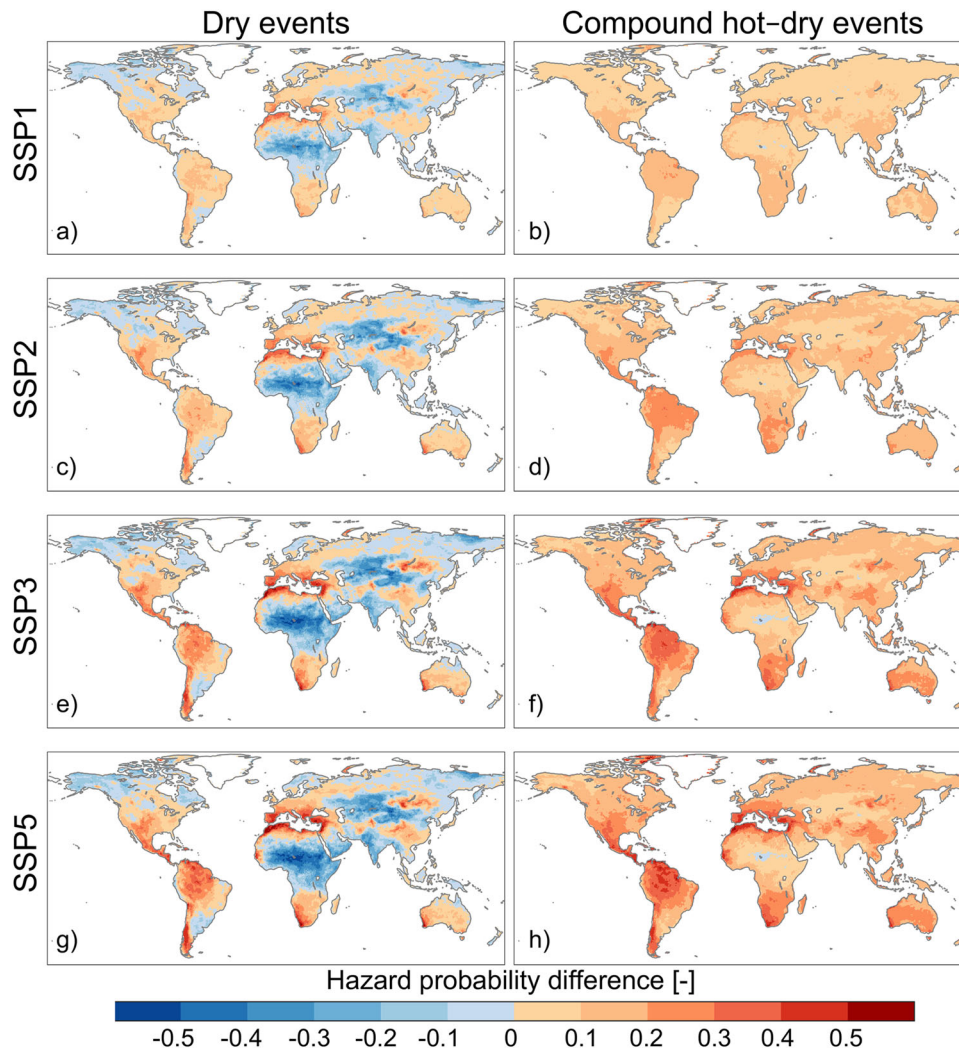


**Fig. 1** Future changes in the occurrence probability of single dry events and compound hot-dry events. Displayed are spatial patterns of CMIP6 multi-model median difference of the occurrence probability of (a, c, e, g) single dry events and (b, d, f, h) compound hot-dry events between the 2061–2100 and 1971–2010 periods for different scenarios. Compound hot-dry events were derived using the Gaussian copula. Results for compound hot-dry events derived using the Gumbel and Clayton copulas are presented in Supplementary Figs. 2 and 3, respectively.

## RESULTS

### Impact of climate change on compound hot-dry events compared to single dry events

To investigate whether climate change has a more severe impact on compound hot-dry events compared to single dry events, we compare the expected changes in the probability of each type of event for the four ScenarioMIP Tier 1 scenarios (SSP1–2.6, SSP2–4.5, SSP3–7.0, and SSP5–8.5, hereafter referred to as SSP1, SSP2, SSP3, and SSP5) (Fig. 1). Our results show that while the occurrence probability of single dry events is expected to increase in approximately 50% of the global land area, the affected area significantly increases for compound hot-dry events due to a large widespread increase in the probability of hot extremes covering the entire globe. The increase in the probability of compound hot-dry events is statistically significant ( $P$  value  $< 0.05$ ) worldwide except for small regions in central Africa and central Asia (Supplementary Fig. 1).

Although the spatial pattern of changes in occurrence probability remains constant across SSP scenarios, its magnitude enlarges with the SSP scenario, particularly for compound events. The global land area with an increase in occurrence probability of

single and compound events is respectively within the ranges of 47.6–53% and 99.3–99.8%. The global median of the magnitude of the increase in the occurrence probability of dry events ranges from 0.05 to 0.10 for SSP1, SSP2, SSP3, and SSP5, respectively, while for compound hot-dry events, the magnitude of increase ranges from 0.09 to 0.17 for the respective SSPs. The Mediterranean, western and central Europe, Central and South America, southern Africa, and eastern Asia exhibit the largest and most significant increases (signal-to-noise  $> 3$ ) in the probability of compound events, as shown in Fig. 1 and Supplementary Fig. 1. Notably, the signal-to-noise ratio for compound events is much larger than that for single events, owing to greater climate change signals for compound events (Supplementary Fig. 1).

In areas where the probability of single dry events is projected to increase, the probability of compound hot-dry events is also projected to rise (Fig. 1). This increase is driven by an increase in the occurrence probability of both hot and dry events. In such areas, the contribution of hot events is more significant for the SSP1 scenario, whereas the contribution of dry events increases with higher SSPs and becomes larger than that of hot events for SSP3 and SSP5. Conversely, in areas where the probability of single

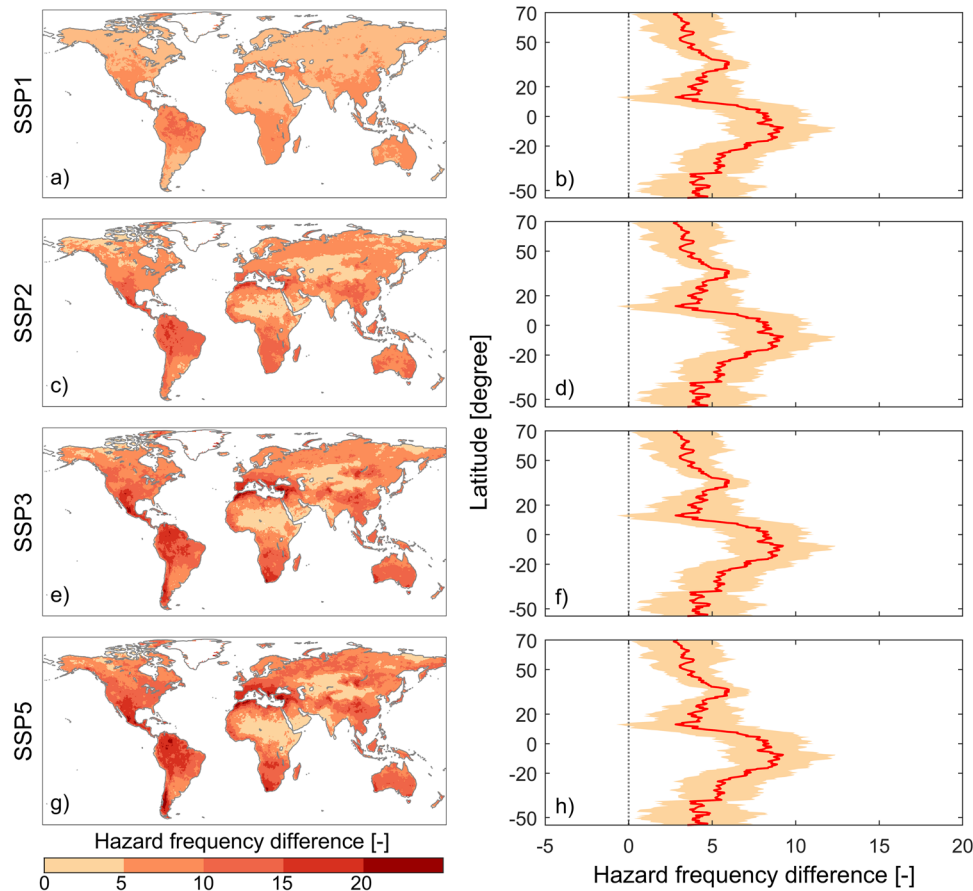


**Fig. 2 Future changes in the frequency of compound hot-dry events.** Displayed are spatial patterns of the difference in frequency between the 2061–2100 and 1971–2010 periods based on the CMIP6 ensemble median (**a, c, e, g**) and the latitudinal distribution of the range of changes across GCMs (**b, d, f, h**). In right-column panels, lines and uncertainty bands represent the ensemble median and  $\pm 1$  ensemble standard deviation, respectively. Compound hot-dry events were derived using the Gaussian copula.

dry events is projected to decrease, the probability of compound hot-dry events still increases due to the projected rise in hot events.

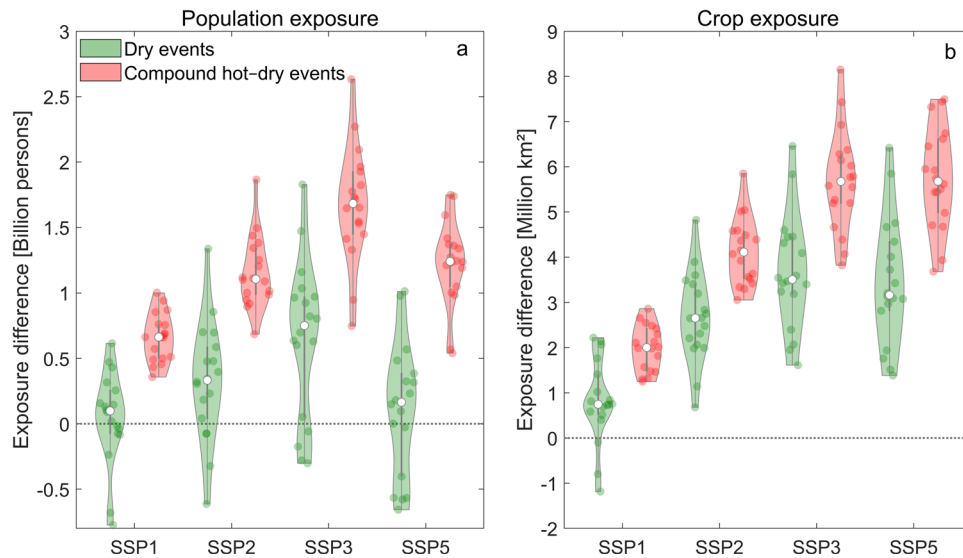
Figure 1 presents the results obtained from applying the Gaussian copula to characterize compound hot-dry events. To assess the impact of using different copula functions on the results, we also employed the Gumbel and Clayton copulas to model these events, and the corresponding results are depicted in Supplementary Figs. 2 and 3, respectively. The results from these copulas exhibit comparable spatial patterns and magnitudes of changes in the probability of compound events to those obtained using the Gaussian copula. Therefore, we concluded that the results are not highly sensitive to the choice of copula functions, and we used the compound events characterized by only the Gaussian copula in subsequent analyses. Previous studies also reported similar findings, demonstrating that the differences resulting from the use of different copula functions were negligible when considering changes in drought characteristics at large scales<sup>39</sup>.

Figure 2 shows the expected changes in the frequency of compound hot-dry events. Based on the global median of the changes, compound hot-dry events are expected to occur 4, 7, 9, and 10 times more frequently in the future under SSP1, SSP2, SSP3, and SSP5 scenarios, respectively. In addition to the variation of climate change impacts with SSPs, the impacts also vary latitudinally, with the largest increase in the tropical and subtropical regions in the Southern Hemisphere.

### Projected croplands and population exposure to single and compound hot-dry events

The impacts of more prevalent and frequent single and compound events in the future on croplands and population are quantified by computing the changes in their exposure to these events between the late twentieth and twenty-first centuries (Fig. 3). The population exposure to dry events, defined as the product of the exposed population and the probability of the events, is projected to increase by 0.1, 0.3, 0.8, and 0.2 billion persons for SSP1, SSP2, SSP3, and SSP5, respectively (Fig. 3a). However, compound hot-dry events are expected to result in much larger increases in population exposure, accounting for 0.7, 1.1, 1.7, and 1.2 billion persons increases for the respective scenarios. The large increases in population exposure are driven by both the increase in the probability of these events (Fig. 1) and the projected population growth, especially for Africa and southern Asia (Supplementary Fig. 4).

The cropland exposure to single and compound events is expected to increase by comparable magnitudes to the population exposure. The exposure of croplands to single dry events, defined as the product of exposed cropland and the probability of hazards, is projected to increase by 0.7, 2.7, 3.5, and 3.2 million km<sup>2</sup> for SSP1, SSP2, SSP3, and SSP5, respectively. For compound hot-dry events, the increase in cropland exposure is expected to be even greater, with projected increases of 2, 4.1, 5.7, and 5.7 million km<sup>2</sup> for the respective scenarios (Fig. 3b). The low crop exposure under SSP1 is attributed to minimal changes in both croplands and compound events, although the expansion of



**Fig. 3 Comparison of future changes in exposure to single dry events and compound hot-dry events.** Displayed is the difference in **a** total population and **b** total cropland exposures between historical and future periods. Green and red dots represent the changes derived from individual CMIP6 GCMs for single and compound events, respectively; the white dot represents the CMIP6 ensemble median.

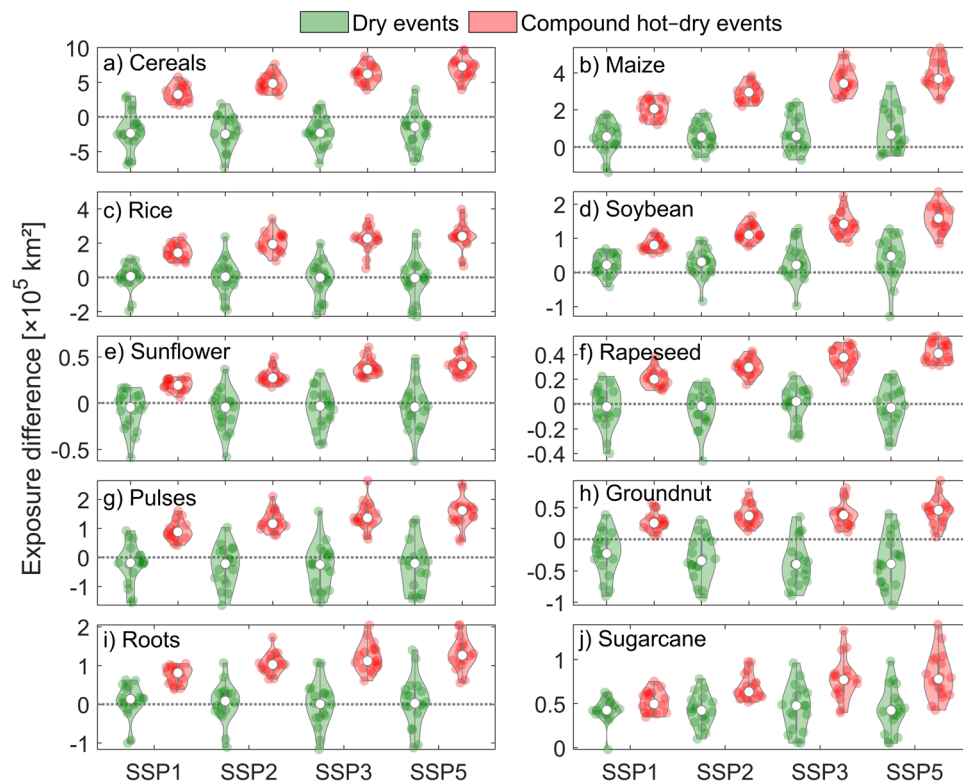


**Fig. 4 Comparison of future changes in exposure of different crops to single dry events and compound hot-dry events.** Displayed are the cropland exposure difference between historical and future periods for **a–j** different crops. Green and red dots represent the changes derived from individual CMIP6 GCMs for single dry events and compound hot-dry events, respectively; the white dot represents the CMIP6 ensemble median.

croplands in some regions such as Sub-Saharan Africa and India is noticeable (Supplementary Fig. 5). In contrast, under the SSP2 and SSP3 scenarios, the largest cropland expansions are anticipated in Sub-Saharan Africa, India, the eastern USA, and parts of South America. The cropland expansion is generally smaller under SSP5 compared to SSP2 and SSP3 except in US and Europe where cropland expansions are largest under SSP5.

The analysis of cropland exposure to hazards for major crops reveals that compound hot-dry events are expected to impact all crop types, while the impact of single dry events is less significant (Fig. 4). The exposure of cereals to compound events is projected to increase by 0.32, 0.48, 0.62, and 0.73 million km<sup>2</sup> for SSP1, SSP2, SSP3, and SSP5, respectively. For oil crops, the magnitudes of the increases in exposure to compound events are 0.21, 0.28, 0.35, and

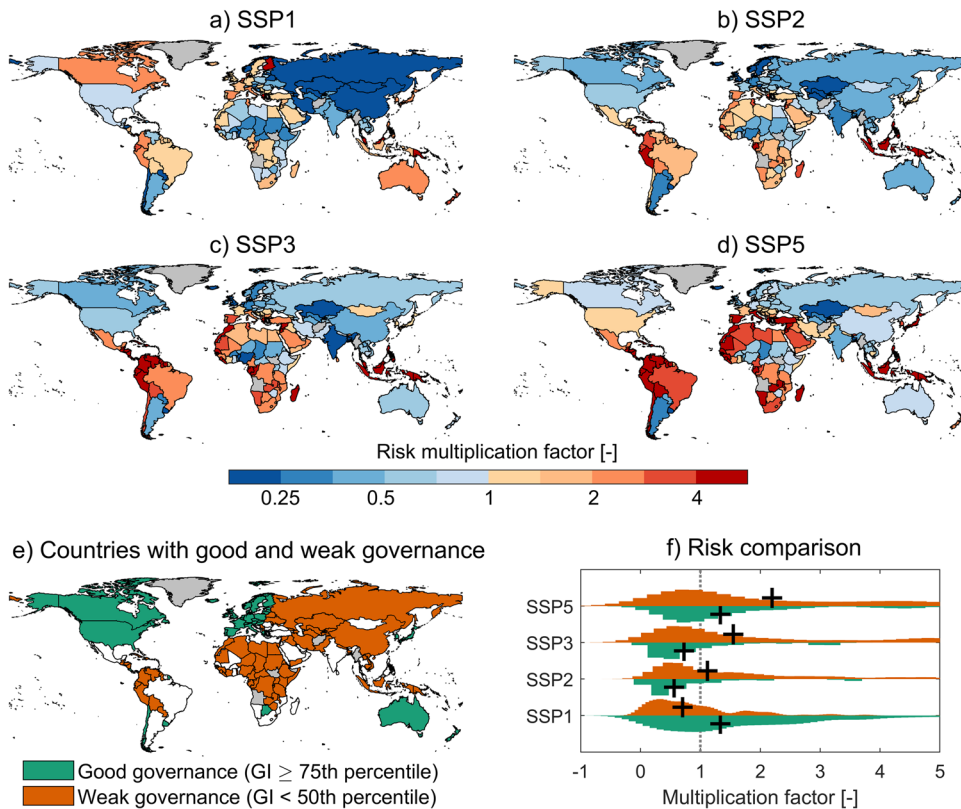


**Fig. 5** Future changes in the risk of compound hot-dry events. Displayed are (a–d) spatial patterns of the risk factor for compound hot-dry events between historical and future periods, (e, f) risk factor comparison between countries with good and weak governance. Hazard change is based on the CMIP6 multi-model median. In panel e, countries with medium governance (50th–74th percentile<sup>31</sup>), which are not used in this study, are shown in white color. In the violin plots, the black cross represents the risk factor median across the countries.

0.40 million km<sup>2</sup> for the respective scenarios. Among the crops considered, the largest increases in exposure to compound events are projected for maize, rice, pulses, soybean, roots, and sugarcane, respectively, while the increases are lowest for sunflower, rapeseed, and groundnut (Fig. 4). The largest increase in maize cultivation areas is expected in Sub-Saharan Africa and South America, while the largest expansion in paddy fields is projected for southern Asia (Supplementary Fig. 6). Groundnut and pulses cultivation are expected to expand largely in Sub-Saharan Africa, southern Asia, and parts of South America (Supplementary Fig. 6). The greatest differences between the changes in exposure to single and compound events are found for cereals, groundnut, and pulses, which exhibit an opposite direction of change (Fig. 4). In terms of change magnitude, the largest difference between single and compound events is projected for cereals. Sub-Saharan Africa, Argentina, and India are anticipated to have the largest increases in cereals-growing areas in the future.

### Country-level assessment of compound hot-dry event risks and contributing factors

The risk of compound hot-dry events is assessed at the country level after aggregating exposure and hazard and integrating with the country-level GI (Supplementary Fig. 7) in this study. The risk analysis shows an increasing trend in 72, 80, 95, and 112 countries out of the total 157 considered countries for SSP1, SSP2, SSP3, and SSP5, respectively (Fig. 5). For the respective scenarios, a fourfold increase in the risk of compound events is found in 11, 22, 45, and 55 countries. The median risk multiplication factors across all 157 countries are 0.9, 1.1, 1.6, and 2.3 for SSP1, SSP2, SSP3, and SSP5, respectively. The Caribbean countries (Jamaica, Trinidad and

Tobago, and Puerto Rico) are the most impacted countries across all SSP scenarios. A comparison of risk between countries with good (governance indicator  $\geq 0.75$ ) and weak (governance indicator  $< 0.5$ ) governance indicates a larger increasing tendency of risk in countries with weak governance, with the exception of SSP1. The changes in the risk of compound events in countries with weak governance are expected to be almost twice as large as those in countries with good governance. The risk multiplication factors of 0.6, 0.7, and 1.3 respectively for SSP2, SSP3, and SSP5 in countries with good governance increase to 1.2, 1.6, and 2.2 for the respective scenarios in countries with weak governance.

The factors driving changes in the risk of compound hot-dry events in each country are examined. Hazard is the primary contributor to risk changes, accounting for global mean contributions of 55%, 68%, 69%, and 69% for SSP1, SSP2, SSP3, and SSP5, respectively (Fig. 6). Hazard has the largest contributions in 108, 139, 140, and 141 countries for SSP1, SSP2, SSP3, and SSP5, respectively. Vulnerability is the second most important driver of risk changes, globally accounting for 35%, 20%, 16%, and 14% for SSP1, SSP2, SSP3, and SSP5, respectively. In individual countries, vulnerability can contribute over 90%. Population and crop exposures have comparable contributions, with the latter slightly larger. Although exposures have the lowest global contributions to risk changes, they can account for up to 66% in individual countries. The contributions of all risk components increase with SSP scenarios except for vulnerability, which has an opposite trend.

### DISCUSSION

The higher occurrence probability of compound hot-dry events in the future compared to single events can be attributed to two

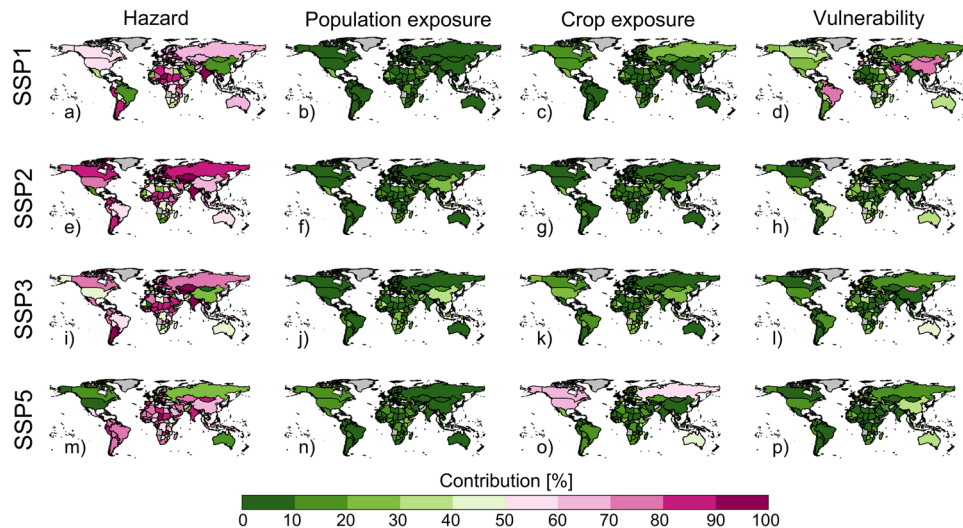


**Fig. 6 Drivers of the change in the risk of compound hot-dry events.** Displayed are the country-level contribution of (a, e, i, m) hazard, (b, f, j, n) population exposure, (c, g, k, o) crop exposure, and (d, h, l, p) vulnerability to the changes in the risk of compound hot-dry events for different scenarios.

factors: an increase in the probability of both dry and hot extreme events<sup>40,41</sup>, and a stronger connection between temperature and soil moisture due to amplification of land-atmosphere feedback and changes in common driving forces such as large-scale atmospheric circulation patterns<sup>34,42,43</sup>. These conditions are met in several regions such as the Mediterranean, western and central Europe, Central and South America, southern Africa, and eastern Asia, leading to a remarkable increase in the probability of compound hot-dry events. This increase is due to a combination of decreased soil moisture<sup>39,44</sup> and increased temperature<sup>45</sup>. In contrast, high-latitude regions exhibit a weaker increase in the probability of compound hot-dry events due to the decreasing trend of dry event probability<sup>39,44</sup>, which offsets the increasing trend of hot event probability<sup>46</sup>. Our findings indicate a substitutional increase in the global exposed area from 50% of the land for single dry events to almost 100% for compound hot-dry events. The increase in the occurrence probability of compound events locally is expected to further expand the exposed area in the future<sup>47</sup>, a trend that has already been observed in the last few decades<sup>48</sup>.

Previous global-scale studies using CMIP5 and CMIP6 GCM simulations<sup>10,13,27,28,49,50</sup> have also reported a significant increase in compound dry and hot events in the future. However, these studies used precipitation as a measure of dry events, which is expected to undergo less change compared to soil moisture<sup>44</sup>. Although a simple threshold approach may not be sufficient to fully characterize the complex interaction between hot and dry events, recent research has shown that using precipitation to define compound hot-dry events results in smaller expected changes compared to when soil moisture is used for this purpose<sup>51</sup>.

Our study reveals that population exposure to compound hot-dry events is projected to increase by 0.7, 1.1, 1.7, and 1.2 billion persons for SSP1, SSP2, SSP3, and SSP5, respectively. The highest population exposure is anticipated under the SSP3 scenario, where the population is expected to increase the most. These findings are in line with our single hazard analyses and previous studies<sup>52</sup>, which also identified SSP3 as the scenario with the highest population exposure to various hazards. Moreover, our results indicate that under the SSP3 scenario's great inequality conditions, the world's poorest populations, especially those in Sub-Saharan Africa and southern Asia, will be disproportionately affected by compound hot-dry events. This conclusion aligns with the IPCC 2018 special report on global warming of 1.5 °C, which

also highlights this threat as a significant risk for vulnerable populations<sup>53</sup>.

Our study also reveals an increase in cropland exposure to compound hot-dry events by 0.7–3.2 million km<sup>2</sup>, depending on the SSP scenario, which is 1.5–2 times greater than the increase in cropland exposure to single dry events. This higher exposure of crops to compound hot-dry events can result in reduced yields, as crops under water stress conditions close their stomata to conserve water, thereby reducing carbon uptake through photosynthesis and ultimately decreasing yields<sup>54</sup>. Additionally, crop yields can sharply decline due to heat stress and increasing water demand during hot events<sup>55</sup>.

This reduced crop yield is particularly concerning as global food demand is expected to double by the 2050s due to projected population growth<sup>56,57</sup>. Our findings reveal a significant increase in cropland exposure to compound hot-dry events in Sub-Saharan Africa, where cereals and roots growing area expansions are associated with a larger cropland exposure. This increase in cropland exposure is of great concern, as Sub-Saharan Africa already faces chronic hunger, with the largest number of food-insecure people in the world<sup>58</sup>, and crop production is vulnerable to water stress conditions due to insufficient contingency planning and limited coping mechanisms<sup>59,60</sup>.

Other regions that will be significantly impacted include South America and India, where the exposure of cereals will be remarkably increased. This trend could have far-reaching impacts on global food security as Brazil and Argentina are the third and fourth largest maize producers in the world, and India produces one-fourth of the world's rice. The projected increase in cropland exposure to compound hot-dry events in these regions underscores the urgent need for proactive measures to address the threats to crop production and food security posed by climate change.

Our study indicates that the risk of compound hot-dry events is expected to increase significantly due to the projected increase in hazard and exposure. Specifically, our findings suggest that the risk of compound hot-dry events is anticipated to increase in 72–112 countries, with a fourfold increase in 11–55 countries, depending on the SSP scenarios considered. Furthermore, we found that countries with weaker governance structures are at higher risk compared to those with good governance, as infrastructural, social, and economic capacities are often insufficient to manage the consequences of disasters. Therefore, it is critical to enhance coping capacities in these countries to reduce

the risk of compound events for society urgently. Educational and economic development are central determinants of improvements in governance efficiency and coping capacities. Economic growth can potentially mitigate the adverse impacts of compound hot-dry events by enabling investment in climate adaptation, research and development, economic diversity, education, and awareness<sup>61</sup>. Furthermore, improving education by increasing awareness of natural hazards can lead to more informed and prepared individuals and communities<sup>21</sup>. This, in turn, can help to reduce the risks and impact of natural disasters, ultimately saving lives and reducing damage to property and infrastructure. International cooperation is critical in addressing the global risks associated with compound events. Countries with higher capacities and resources can support those with weaker governance structures through technology transfer, financial aid, and capacity-building initiatives. Collaborative efforts can also promote the sharing of best practices and knowledge on climate adaptation, disaster risk reduction, and sustainable development.

Our analysis reveals that hazard is the most significant element contributing to the risk multiplication factor compared to population and cropland exposures and vulnerability. Depending on the SSP scenarios, the median contribution of hazard to changes in risk ranges from 55% to 69% globally. However, the contribution of hazard varies considerably across different countries and can be less than 10% in some cases. This underscores the need to consider all three risk elements to avoid biased estimates of the risk of compound events. Failing to do so could result in underestimation or overestimation of the risk, leading to inappropriate policy responses. Our findings have important implications for policymakers, providing valuable information to prioritize adaptation actions and quantitatively determine the level of enhancement needed in each risk component to mitigate the adverse impacts of compound hot-dry events.

This study provides a comprehensive assessment of the global risks associated with compound hot-dry events by incorporating hazard, exposure, and vulnerability indicators. There are several ways in which future research could extend and improve upon the methods and analysis presented here. One important direction for future studies would be to quantify compound hot-dry events for different global warming levels, including the 1.5 and 2 °C targets outlined in the Paris Agreement. This would provide insights into the consequences of meeting or failing to meet these targets and could inform decision-making on mitigation and adaptation strategies.

Another way to improve upon this study would be to develop a vulnerability index specifically designed for the vulnerability assessment of compound hot-dry events. While the governance indicator used in this study covers different relevant dimensions of vulnerability and coping capacity, it was not specifically designed for this purpose. A more comprehensive vulnerability index based on additional proxy indicators, as they become available at a global scale and for different socioeconomic scenarios, could help to better assess the risks of compound hot-dry events and inform adaptation strategies.

Furthermore, it would be valuable to provide risk analysis at smaller scales than the country level, where data on vulnerability and coping capacity are available. This could help to identify areas of high vulnerability within countries, particularly in large developing nations where socioeconomic inequality can be significant. Additionally, future studies could take into account the level of humanitarian assistance needed by the population, based on factors such as health conditions and age dependency. Humans are particularly sensitive to high heat stress due to hot and humid air, and such information could be used to inform disaster preparedness plans and risk reduction strategies.

Despite these potential areas for improvement, the risk assessment of compound hot-dry events presented in this study

provides valuable insights into the potential impacts of climate change and can help to inform informed decision-making on adaptation and risk reduction strategies at national and global scales.

## METHODS

### Hazard quantification

In this study, we define risk as a function of hazard, exposure, and vulnerability/coping-capacity. To model hazard, we used climate simulations from 18 general circulation models (GCMs; Supplementary Table 1) as part of the Coupled Model Intercomparison Project Phase 6 (CMIP6<sup>62</sup>). Specifically, we analyzed monthly soil moisture and air temperature data from 1971 to 2100 under four different socio-economic scenarios: SSP1–2.6, SSP2–4.5, SSP3–7.0, and SSP5–8.5. Based on the CMIP6 ensemble median, these scenarios correspond to projected global warming rates of 2.2, 3.3, 4.3, and 5.1 °C at the end of the century<sup>39</sup>.

To quantify compound hot-dry events (hazard), we transformed soil moisture and temperature series at each grid cell to the series of standardized indices, enabling a comparison of dry and hot conditions across regions and climate scenarios. To this end, we employed the standardized soil moisture index (SSI<sup>63</sup>) and the standardized temperature index (STI<sup>64</sup>) to define dry and hot events, respectively. The nonparametric Gringorten plotting position formula  $P = (i - 0.44)/(n + 0.12)$  ( $n$ : length of the data;  $i$ : rank) was used to derive the marginal probability. We estimated the marginal probability for the entire time series (1971–2100), which enables us to capture any changes in normal conditions (i.e., trends) and anomalies caused by climate change<sup>24,65</sup>.

The dependence between hot and dry events at each grid cell of the CMIP6 GCMs, referring to the tendency of these events to inhibit (negative correlation) or facilitate (positive correlation) each other, was quantified using a bivariate copula. Copula functions are able to characterize the dependence structure independently of the type of marginal distributions and allow a flexible mensuration of the tail dependence<sup>66</sup> as well as the estimation of conditional probabilities<sup>67</sup> which are important for risk analyses of extreme events. As compound hot-dry events usually occur when soil moisture (SSI) is low and air temperature (STI) is high, we inverted the SSI values. The joint distribution probability between inverted 3-month SSI and monthly standardized temperature values was derived using copulas. We considered three popular copula functions: the Gaussian copula, which is part of the elliptical family and assumes multivariate normality; the Gumbel copula, which is from the Archimedean family and assumes upper tail dependence; and the Clayton copula, also from the Archimedean family, which assumes lower tail dependence. These copulas were chosen for their ability to capture different types of dependence between the two variables. To estimate the parameters of these copulas, we used the maximum likelihood method. Following the concepts of SSI, the standardized compound hot-dry event index was obtained by transforming the remapped joint probability derived from copula functions using the standard normal distribution ( $\Phi^{-1}(p)$  where  $\Phi$  is the standard normal distribution and  $p$  is the joint probability).

To ensure a reliable estimation of the copula parameters, a compound hot-dry event was defined as a standardized joint probability below  $-0.5$ , based on previous studies<sup>2,63,68</sup>. This threshold guarantees an adequate number of events for both historical (1971–2010) and future (2061–2100) periods. The probability of occurrence for these events was calculated as the ratio of instances with a compound event to the total number of months in each period (40 years  $\times$  12 months = 480 months). This study focused on the far future period to project changes in compound hot-dry events under different scenarios, reflecting various challenges for implementing mitigation and adaptation

strategies, and global policies<sup>69</sup>. The magnitude of the forced signal varies depending on the scenario, which is more apparent in long-term projections as it is generally greater than the internal variability of the climate system<sup>70</sup>. By utilizing a 40-year period and a lower threshold for defining compound hot-dry events, this study captured a sufficient number of extreme events and increased the sample size, thereby reducing fitting errors due to limited samples. This approach is effective in ensuring a reliable estimation of the parameters of copulas.

To explore the possible larger impact of compound hot-dry events, it was compared with the impact from single events. The bivariate threshold corresponds to a slightly higher threshold for margins because the bivariate threshold in addition to the jointly marginally extreme events also contains the events that are extreme based on the bivariate distribution but not necessarily based on both margins<sup>2</sup>. As in previous studies (e.g., ref. <sup>2</sup>), we, therefore, selected a higher threshold (−0.8) for margins (SSI and STI), although global patterns and magnitude of changes were found insensitive to the threshold for defining extreme events<sup>39</sup>.

We considered the change in hazards as the difference in the occurrence probability of hazards between 2061–2100 and 1971–2010 periods. To assess the robustness of the changes within the context of natural variability, the magnitude of the forced climate response (signal; ensemble median of changes) compared to internal variability (noise; standard deviation across the ensemble) is examined<sup>71</sup>. The statistical significance of the forced response was tested by defining a t-test statistic in terms of the signal-to-noise ratio<sup>72</sup>. For our ensemble size ( $n = 18$ ), the change is considered significant at the 5% level when the absolute value of the signal-to-noise ratio exceeds 0.54.

### Risk assessments

Our risk assessment incorporated population exposure, following similar single-hazard risk studies. We utilized population density data at a spatial resolution of  $0.5^\circ \times 0.5^\circ$  and an annual temporal resolution for historical and future periods (2005 and 2085). The gridded population dataset included historical population density from the HYDE3.2 database<sup>73</sup>, and future population data derived by scaling up the 2010 Gridded Population of the World (GPWv3) dataset (available at <http://sedac.ciesin.columbia.edu/data/collection/gpw-v3>) using national decadal population projections based on SSP1, SSP2, SSP3, and SSP5<sup>74</sup>, which were linearly interpolated to an annual scale. We also considered the exposure of cropland to events for historical and future periods (2005 and 2085), with cropland proportions for different SSPs extracted from gridded land-use data on a  $0.5^\circ \times 0.5^\circ$  grid from the AIM-SSP/RCP Gridded Emissions and Land-use dataset<sup>75</sup>. In the exposure analysis depicted in Figs. 3 and 4, the probability of the hazard at each grid cell was multiplied by the corresponding population and cropland proportion. The percentage of total cropland at each  $0.5^\circ \times 0.5^\circ$  grid cell was converted to square kilometers using spherical trigonometry, which accounts for varying areas of GCM grid cells across latitudes.

For further analysis of cropland exposure to single and compound events, the exposure of 10 predominant crop species and species groups was investigated. Future land use patterns were based on projections from the MAgPIE land-use model<sup>76,77</sup> according to SSP2. In this dataset, to ensure a smooth transition between the historical (HYDE3.2) and future land use patterns, a harmonization algorithm was applied to the MAgPIE data. Future projections of croplands are available for each of the GFDL-ESM2M, HadGEM2-ES, IPSL-CM5A-LR, and MIROC5 GCMs. We calculated the median of the projections for historical and future periods (2005 and 2085) and used it in our study.

In our analysis of vulnerability and adaptive capacity, we used the governance indicator (GI<sup>38</sup>) for the historical period and different SSPs (2005 and 2085). Previous studies have shown that the quality

and efficiency of governance are crucial in the immediate aftermath of extreme events, as well as in the future climate vulnerability and coping capacity of nations to extremes<sup>38,78,79</sup>. This indicator was developed by integrating gross domestic product (GDP) per capita, the share of the population with higher education, and the gender gap in mean years of schooling.

To quantify the risk of compound hot-dry events for the historical period and different SSPs in the future, we aggregated the gridded population and cropland data, as well as the gridded hazard probability, to the country level. To calculate the overall exposure to compound hot-dry events at each grid cell, we integrated the cropland proportion with the population exposure of the same grid, which were normalized using linear min-max rescaling between 0.05 (lowest) and 0.95 (highest) before the integration. Since there is an indirect relationship between governance indicator (GI) and risk (where lower GI values indicate higher vulnerability), we used one minus GI for risk analysis. Risk was determined as the product of normalized hazard, integrated exposure, and vulnerability. We calculated the risk multiplication factor as the ratio of the risk in the future period over that in the historical period. This factor was disentangled into changes in hazard, population and crop exposures, and vulnerability, providing valuable insights for prioritizing adaptation actions.

### DATA AVAILABILITY

The CMIP6 soil moisture and air temperature data used in this study are accessible online through the Earth System Grid Federation (ESGF) system. The population and land use data (Landuse 15 Crops) are also available on the ESGF website. Additionally, the AIM-SSP/RCP Gridded Emissions and Land-use dataset can be obtained at [https://www-iam.nies.go.jp/aim/data\\_tools/aimssp/aimssp.html](https://www-iam.nies.go.jp/aim/data_tools/aimssp/aimssp.html).

### CODE AVAILABILITY

The codes used in this study are available on request from the corresponding author (hossein.tabari@uantwerpen.be).

Received: 10 November 2022; Accepted: 14 June 2023;

Published online: 24 June 2023

### REFERENCES

- Zscheischler, J. et al. A typology of compound weather and climate events. *Nat. Rev. Earth Environ.* **1**, 333–347 (2020).
- Brunner, M. I., Gilleland, E. & Wood, A. W. Space–time dependence of compound hot–dry events in the United States: assessment using a multi-site multi-variable weather generator. *Earth Syst. Dyn.* **12**, 621–634 (2021).
- IPCC. Weather and climate extreme events in a changing climate, Climate Change 2021: The Physical Science Basis. Contribution of Working Group I to the Sixth Assessment Report of the Intergovernmental Panel on Climate Change (ed.: S. I. Seneviratne and X. Zhang) (2021).
- WMO. Atlas of Mortality and Economic Losses from Weather, Climate and Water Extremes (1970–2019). WMO-No. 1267 (2021).
- Hoag, H. Russian summer tops ‘universal’ heatwave index. *Nature* **16**, 636 (2014).
- Munich R. E. Heatwaves, Drought, and Forest Fires in Europe: Billions of Dollars in Losses for Agricultural Sector. Munich: Munich Re., Available from: <https://www.munichre.com/topics-online/en/climate-change-and-natural-disasters/climate-change/heatwaves-and-drought-in-europe.html> (2020).
- Wegren, S. K. Food security and Russia’s 2010 drought. *Eurasia. Geogr. Econ.* **52**, 140–156 (2011).
- Christian, J. I., Basara, J. B., Hunt, E. D., Otkin, J. A. & Xiao, X. Flash drought development and cascading impacts associated with the 2010 Russian heatwave. *Environ. Res. Lett.* **15**, 094078 (2020).
- Mehrabi, Z. & Ramankutty, N. Synchronized failure of global crop production. *Nat. Ecol. Evol.* **3**, 780–786 (2019).
- Liu, W. et al. Future climate change significantly alters interannual wheat yield variability over half of harvested areas. *Environ. Res. Lett.* **16**, 094045 (2021).
- Sarhadi, A., Ausin, M. C., Wiper, M. P., Touma, D. & Diffenbaugh, N. S. Multi-dimensional risk in a nonstationary climate: Joint probability of increasingly severe warm and dry conditions. *Sci. Adv.* **4**, eaau3487 (2018).



12. Ridder, N. N. et al. Global hotspots for the occurrence of compound events. *Nat. Commun.* **11**, 1–10 (2020).
13. Wu, X. et al. Projected increase in compound dry and hot events over global land areas. *Int. J. Climatol.* **41**, 393–403 (2021).
14. Mukherjee, S. & Mishra, A. K. Increase in compound drought and heatwaves in a warming world. *Geophys. Res. Lett.* **48**, e2020GL090617 (2021).
15. Bevacqua, E., Zappa, G., Lehner, F. & Zscheischler, J. Precipitation trends determine future occurrences of compound hot-dry events. *Nat. Clim. Change* **12**, 350–355 (2022).
16. Tabari, H. & Willems, P. More prolonged droughts by the end of the century in the Middle East. *Environ. Res. Lett.* **13**, 104005 (2018).
17. Ranasinghe, R. et al. Climate change 1 information for regional impact and for risk assessment. Chapter 12 of The Physical Science Basis. Contribution of Working Group I to the Sixth Assessment Report of the Intergovernmental Panel on Climate Change (ed.: S. I. Seneviratne and X. Zhang) (2021).
18. Knorr, W., Arneht, A. & Jiang, L. Demographic controls of future global fire risk. *Nat. Clim. Change* **6**, 781–785 (2016).
19. Alfieri, L., Feyen, L., Dottori, F. & Bianchi, A. Ensemble flood risk assessment in Europe under high end climate scenarios. *Glob. Environ. Change* **35**, 199–212 (2015).
20. Jongman, B. et al. Declining vulnerability to river floods and the global benefits of adaptation. *Proc. Natl. Acad. Sci.* **112**, E2271–E2280 (2015).
21. Hosseinzadehtalaei, P., Tabari, H. & Willems, P. Satellite-based data driven quantification of pluvial floods over Europe under future climatic and socio-economic changes. *Sci. Total Environ.* **721**, 137688 (2020).
22. Ward, P. J. et al. Natural hazard risk assessments at the global scale. *Nat. Haz. Earth Syst. Sci.* **20**, 1069–1096 (2020).
23. Russo, S. et al. Half a degree and rapid socioeconomic development matter for heatwave risk. *Nat. Commun.* **10**, 1–9 (2019).
24. Tabari, H., Hosseinzadehtalaei, P., Thiery, W. & Willems, P. Amplified drought and flood risk under future socioeconomic and climatic change. *Earth's Future* **9**, e2021EF002295 (2021).
25. Liu, Y. & Chen, J. Future global socioeconomic risk to droughts based on estimates of hazard, exposure, and vulnerability in a changing climate. *Sci. Total Environ.* **751**, 142159 (2021).
26. Zscheischler, J. et al. Future climate risk from compound events. *Nat. Clim. Change* **8**, 469–477 (2018).
27. Meng, Y., Hao, Z., Feng, S., Zhang, X. & Hao, F. Increase in compound dry-warm and wet-warm events under global warming in CMIP6 models. *Glob. Planet. Change* **210**, 103773 (2022).
28. Zhang, G. et al. Climate change determines future population exposure to summertime compound dry and hot events. *Earth's Future* **10**, e2022EF003015 (2022).
29. Burke, E. J. & Brown, S. J. Evaluating uncertainties in the projection of future drought. *J. Hydrometeorol.* **9**, 292–299 (2008).
30. Vicente-Serrano, S. M., Beguería, S. & López-Moreno, J. I. A multiscale drought index sensitive to global warming: the standardized precipitation evapotranspiration index. *J. Clim.* **23**, 1696–1718 (2010).
31. Milly, P. C. & Dunne, K. A. Potential evapotranspiration and continental drying. *Nat. Clim. Change* **6**, 946–949 (2016).
32. Greve, P., Roderick, M. L., Ukkola, A. M. & Wada, Y. The aridity index under global warming. *Environ. Res. Lett.* **14**, 124006 (2019).
33. EU Science Hub. Summer drought keeps its grip on Europe. Available at [https://joint-research-centre.ec.europa.eu/jrc-news/summer-drought-keeps-its-grip-europe-2022-08-22\\_en](https://joint-research-centre.ec.europa.eu/jrc-news/summer-drought-keeps-its-grip-europe-2022-08-22_en) (2022).
34. Seneviratne, S. I. et al. Investigating soil moisture–climate interactions in a changing climate: A review. *Earth-Sci. Rev.* **99**, 125–161 (2010).
35. West, H., Quinn, N. & Horswell, M. Remote sensing for drought monitoring & impact assessment: Progress, past challenges and future opportunities. *Remote Sens. Environ.* **232**, 111291 (2019).
36. Berg, A., Sheffield, J. & Milly, P. C. Divergent surface and total soil moisture projections under global warming. *Geophys. Res. Lett.* **44**, 236–244 (2017).
37. Cook, B. I., Mankin, J. S. & Anchukaitis, K. J. Climate change and drought: From past to future. *Curr. Clim. Change Rep.* **4**, 164–179 (2018).
38. Andrijevic, M., Cuaresma, J. C., Muttarak, R. & Schleussner, C. F. Governance in socioeconomic pathways and its role for future adaptive capacity. *Nat. Sustain.* **3**, 35–41 (2020).
39. Tabari, H. & Willems, P. Trivariate analysis of changes in drought characteristics in the CMIP6 multi-model ensemble at global warming levels of 1.5, 2 and 3 °C. *J. Clim.* **35**, 5823–5837 (2022).
40. Zscheischler, J. & Seneviratne, S. I. Dependence of drivers affects risks associated with compound events. *Sci. Adv.* **3**, e1700263 (2017).
41. De Luca, P., Messori, G., Faranda, D., Ward, P. J. & Coumou, D. Compound warm–dry and cold–wet events over the Mediterranean. *Earth Syst. Dyn.* **11**, 793–805 (2020).
42. Kopp, R., Easterling, D. R. and Hall, T. Potential surprises—compound extremes and tipping elements. In: Wuebbles, D. W. F. D. J., Hibbard, K. A., Dokken, D. J., Stewart, B. C. and Maycock, T. K. (Eds.) Climate Science Special Report: Fourth National Climate Assessment. Washington, DC: U.S. Global Change Research Program, pp. 411–429 (2017).
43. Kornhuber, K. et al. Extreme weather events in early summer 2018 connected by a recurrent hemispheric wave-7 pattern. *Environ. Res. Lett.* **14**, 054002 (2019).
44. Cook, B. I. et al. Twenty-first century drought projections in the CMIP6 forcing scenarios. *Earth's Future* **8**, e2019EF001461 (2020).
45. Tebaldi, C. et al. Climate model projections from the scenario model inter-comparison project (ScenarioMIP) of CMIP6. *Earth Syst. Dyn.* **12**, 253–293 (2021).
46. Fan, X., Duan, Q., Shen, C., Wu, Y. & Xing, C. Global surface air temperatures in CMIP6: historical performance and future changes. *Environ. Res. Lett.* **15**, 104056 (2020).
47. Vogel, M. M., Zscheischler, J., Wartenburger, R., Dee, D. & Seneviratne, S. I. Concurrent 2018 hot extremes across Northern Hemisphere due to human-induced climate change. *Earth's Future* **7**, 692–703 (2019).
48. Alizadeh, M. R. et al. A century of observations reveals increasing likelihood of continental-scale compound dry-hot extremes. *Sci. Adv.* **6**, eaaz4571 (2020).
49. Vogel, M. M., Hauser, M. & Seneviratne, S. I. Projected changes in hot, dry and wet extreme events' clusters in CMIP6 multi-model ensemble. *Environ. Res. Lett.* **15**, 094021 (2020).
50. Ridder, N. N., Ukkola, A. M., Pitman, A. J. & Perkins-Kirkpatrick, S. E. Increased occurrence of high impact compound events under climate change. *npj Clim. Atmos. Sci.* **5**, 3 (2022).
51. Feng, S., Hao, Z., Zhang, Y., Zhang, X. & Hao, F. Amplified future risk of compound droughts and hot events from a hydrological perspective. *J. Hydrol.* **617**, 129143 (2023).
52. Arnell, N. W. et al. The global and regional impacts of climate change under representative concentration pathway forcings and shared socioeconomic pathway socioeconomic scenarios. *Environ. Res. Lett.* **14**, 084046 (2019).
53. Hoegh-Guldberg, O. et al. Impacts of 1.5°C Global Warming on Natural and Human Systems, in: Masson-Delmotte, V., et al. (Eds.), Global Warming of 1.5°C. An IPCC Special Report on the Impacts of Global Warming of 1.5°C above Pre-Industrial Levels and Related Global Greenhouse Gas Emission Pathways, in the Context of Strengthening the Global Response to the Threat of Climate Change., Intergovernmental Panel on Climate Change (2018).
54. Leng, G. & Hall, J. Crop yield sensitivity of global major agricultural countries to droughts and the projected changes in the future. *Sci. Total Environ.* **654**, 811–821 (2019).
55. Lesk, C. et al. Stronger temperature–moisture couplings exacerbate the impact of climate warming on global crop yields. *Nat. Food* **2**, 683–691 (2021).
56. Godfray, H. C. J. et al. Food security: the challenge of feeding 9 billion people. *Science* **327**, 812–818 (2010).
57. Tilman, D., Balzer, C., Hill, J. & Befort, B. L. Global food demand and the sustainable intensification of agriculture. *Proc. Natl. Acad. Sci.* **108**, 20260–20264 (2011).
58. FAO, ECA and AUC. Africa regional overview of food security and nutrition 2019 (Accra: Food & Agriculture Organization) p 104 (2020).
59. Hadebe, S. T., Modi, A. T. & Mabhaudhi, T. Drought tolerance and water use of cereal crops: A focus on sorghum as a food security crop in sub-Saharan Africa. *J. Agron. Crop Sci.* **203**, 177–191 (2017).
60. Kamali, B., Abbaspour, K. C., Wehrli, B. & Yang, H. Drought vulnerability assessment of maize in Sub-Saharan Africa: Insights from physical and social perspectives. *Glob. Planet Change* **162**, 266–274 (2018).
61. Liu, H., Alharthi, M., Atil, A., Zafar, M. W. & Khan, I. A non-linear analysis of the impacts of natural resources and education on environmental quality: Green energy and its role in the future. *Resour. Policy* **79**, 102940 (2022).
62. Eyring, V. et al. Overview of the Coupled Model Intercomparison Project Phase 6 (CMIP6) experimental design and organization. *Geosci. Model Dev.* **9**, 1937–1958 (2016).
63. Hao, Z. & AghaKouchak, A. Multivariate standardized drought index: a parametric multi-index model. *Adv. Water Resour.* **57**, 12–18 (2013).
64. Zscheischler, J. et al. Impact of large-scale climate extremes on biospheric carbon fluxes: An intercomparison based on MsTMIP data. *Glob. Biogeochem. Cycles* **28**, 585–600 (2014).
65. Spinoni, J. et al. Future global meteorological drought hot spots: A study based on CORDEX data. *J. Clim.* **33**, 3635–3661 (2020).
66. Serinaldi, F., Bonaccorso, B., Cancelliere, A. & Grimaldi, S. Probabilistic characterization of drought properties through copulas. *Phys. Chem. Earth* **34**, 596–605 (2009).
67. Ribeiro, A. F., Russo, A., Gouveia, C. M. & Páscoa, P. Copula-based agricultural drought risk of rainfed cropping systems. *Agric. Water Manag.* **223**, 105689 (2019).

68. Gu, L. et al. Projected increases in magnitude and socioeconomic exposure of global droughts in 1.5 and 2 C warmer climates. *Hydrol. Earth Syst. Sci.* **24**, 451–472 (2020).
69. O'Neill, B. C. et al. The scenario model intercomparison project (ScenarioMIP) for CMIP6. *Geosci. Model Dev.* **9**, 3461–3482 (2016).
70. Collins, M. et al. Long-term climate change: Projections, commitments and irreversibility. In T. F. Stocker, et al. (Eds.), *Climate change 2013: The Physical Science Basis*, 1029–1136 (2013).
71. Kendon, E. J., Rowell, D. P., Jones, R. G. & Buonomo, E. Robustness of future changes in local precipitation extremes. *J. Clim.* **21**, 4280–4297 (2008).
72. Aalbers, E. E., Lenderink, G., van Meijgaard, E. & van den Hurk, B. J. Local-scale changes in mean and heavy precipitation in Western Europe, climate change or internal variability? *Clim. Dyn.* **50**, 4745–4766 (2018).
73. Klein Goldewijk, K., Beusen, A., Doelman, J. & Stehfest, E. Anthropogenic land use estimates for the Holocene–HYDE 3.2. *Earth Syst. Sci. Data* **9**, 927–953 (2017).
74. Samir, K. C. & Lutz, W. Demographic scenarios by age, sex and education corresponding to the SSP narratives. *Popul. Environ.* **35**, 243–260 (2014).
75. Fujimori, S., Hasegawa, T., Ito, A., Takahashi, K. & Masui, T. Gridded emissions and land-use data for 2005–2100 under diverse socioeconomic and climate mitigation scenarios. *Sci. Data* **5**, 1–13 (2018).
76. Popp, A. et al. Land-use protection for climate change mitigation. *Nat. Clim. Change* **4**, 1095–1098 (2014).
77. Stevanović, M. et al. The impact of high-end climate change on agricultural welfare. *Sci. Adv.* **2**, e1501452 (2016).
78. Harrington, L. J., Schleussner, C. F. & Otto, F. E. Quantifying uncertainty in aggregated climate change risk assessments. *Nat. Commun.* **12**, 1–10 (2021).
79. Klein, R. J. T. et al. Adaptation opportunities, constraints, and limits. In: *Climate Change 2014: Impacts, Adaptation, and Vulnerability. Part A: Global and Sectoral Aspects. Contribution of Working Group II to the Fifth Assessment Report of the Intergovernmental Panel on Climate Change* (eds. Field, C. B. et al.), Cambridge University Press, 899–943 (2014).

## AUTHOR CONTRIBUTIONS

The research was designed by H.T. who also performed the statistical analyses, produced display items, and wrote the paper. P.W. contributed to the review of the initial and revised versions of the paper.

## COMPETING INTERESTS

The authors declare no competing interests.

## ADDITIONAL INFORMATION

**Supplementary information** The online version contains supplementary material available at <https://doi.org/10.1038/s41612-023-00401-7>.

**Correspondence** and requests for materials should be addressed to Hossein Tabari.

**Reprints and permission information** is available at <http://www.nature.com/reprints>

**Publisher's note** Springer Nature remains neutral with regard to jurisdictional claims in published maps and institutional affiliations.



**Open Access** This article is licensed under a Creative Commons Attribution 4.0 International License, which permits use, sharing, adaptation, distribution and reproduction in any medium or format, as long as you give appropriate credit to the original author(s) and the source, provide a link to the Creative Commons license, and indicate if changes were made. The images or other third party material in this article are included in the article's Creative Commons license, unless indicated otherwise in a credit line to the material. If material is not included in the article's Creative Commons license and your intended use is not permitted by statutory regulation or exceeds the permitted use, you will need to obtain permission directly from the copyright holder. To view a copy of this license, visit <http://creativecommons.org/licenses/by/4.0/>.

© The Author(s) 2023